

Structure, chromosome localization, and tissue distribution of the mouse *twik* K⁺ channel gene

Isabelle Arrighi^a, Florian Lesage^a, Jean-Claude Scimeca^b, Georges F. Carle^b,
Jacques Barhanin^{a,*}

^aInstitut de Pharmacologie Moléculaire et Cellulaire, CNRS UPR 411, 660 route des Lucioles, Sophia Antipolis, 06560 Valbonne, France

^bUMR 6549 CNRS/UNSA, Faculté de Médecine, Avenue de Valombrose, 06107 Nice cedex 02, France

Received 19 January 1998; revised version received 19 February 1998

Abstract We have recently discovered a new class of potassium channels with two pore-forming domains and four membrane-spanning domains. When heterologously expressed, these channels produce time- and voltage-independent currents that classify them as background or leak channels. TWIK (for tandem of P domains in a weak inwardly rectifying K⁺ channel) was the first member of this family to be cloned. Here, we describe the genomic organization of TWIK in the mouse. The coding sequence as well as the untranslated sequences are contained in three exons. The *twik* gene (or KCNK1) has been mapped to chromosome 8, consistent with its localization to 1q42–43 in human. The *twik* gene is expressed in virtually all mouse tissues. It is most abundantly expressed in brain and moderately in other organs such as kidney. The level of expression is increased in brain and kidney from neonate to adult animals, but the TWIK message is also detected during embryogenesis, as early as day 7 post conception.

© 1998 Federation of European Biochemical Societies.

Key words: Mouse chromosome 8; Background conductance; Development

1. Introduction

Potassium channels are present in virtually all living cells [1,2]. They are exceptionally diverse in their biophysical properties, pharmacology, regulation and tissue distribution. This diversity makes them ideally suited for a large repertoire of functions. K⁺ channels influence action potential waveforms, firing frequency and neurotransmitter secretion, playing a major role in neuronal integration, muscle contraction and heart beating. They also act on hormone secretion, cell volume regulation, ion flow and, potentially, in cell proliferation and differentiation.

K⁺ channels are oligomers of pore-forming subunits often associated with membrane or cytoplasmic auxiliary subunits. Three different families of pore-forming subunits have been cloned in mammals. The *Shaker* family is the most extended class with more than 25 genes recognized to date [3–8]. These genes encode proteins that all contain a hydrophobic core with six transmembrane segments (TMS) and a short region called the P domain involved in the formation of the pore selective to K⁺ [9]. Expression of *Shaker* subunits produces voltage-gated (Kv) or Ca²⁺-activated (KCa) K⁺ channels. The family of inward rectifier K⁺ channels (IRK) comprises 14 genes to date encoding subunits with two TMS and one P

domain [10–12]. They include the inward rectifier (IRK), G-protein-coupled (GIRK) and ATP-sensitive (KATP) K⁺ channels. Finally, the last family of pore-forming subunits that has been identified is the class of K⁺ channels with two P domains. The three different subunits already cloned in human and mouse have four TMS and two P domains [13–15]. When expressed in COS cells and *Xenopus* oocytes, these subunits produce K⁺-selective currents that are instantaneous, non-inactivating and voltage-independent. These characteristics are classical criteria used to describe the leak or background K⁺ channels. These channels are involved in the setting and the modulation of the resting membrane potential of many cell types.

TWIK is the founding member of the 4TMS/2P family of K⁺ channels [13]. It is a 336 amino acid subunit that forms disulfide-bridged homodimers in the brain [16]. When expressed in *Xenopus* oocytes, TWIK produces mildly inwardly rectifying, instantaneous and non-inactivating K⁺ currents. Nothing is known about the organization of genes encoding the new 4TMS/2P K⁺ channels subunits. Here, we report the genomic characterization of TWIK in the mouse, as well as its chromosomal localization and tissue distribution during development.

2. Materials and methods

2.1. 129 Sv/J library screening

A mouse 129 Sv/J genomic library constructed in Lambda Fix phage [17] was screened at high stringency with a α -³²P-labeled probe (10⁶ cpm/ml) corresponding to the coding sequence of TWIK. From 4 × 10⁵ plaques screened, five different positive clones were obtained. One of them was fully characterized by Southern blot analysis and different fragments were subcloned into pBluescript II SK[−] (Stratagene) for subsequent mapping. None of these positive clones contained the 5' part of TWIK. A specific 5' probe of 350 bp was then used to rescreen the library. Two positive clones were identified that contained a total of ~30 kbp DNA contiguous sequence with only ~4 kbp in common that included exon 1. Fragments of the genomic DNA and the exon-intron boundaries were sequenced using the dye terminator technique and an automatic sequencer (Applied Biosystems, model 373A).

2.2. Southern blot analysis

Genomic DNA was isolated from 129 Sv/J mouse liver and digested by a panel of restriction enzymes. Approximately 20 µg of digested genomic DNA was loaded per lane and separated by electrophoresis on 0.8% agarose gel. DNA was transferred to a nylon membrane (Hybond N⁺, Amersham), hybridized with the whole mouse TWIK cDNA α -³²P-labeled probe and exposed to Kodak X-OMAT AR film for 8 days at −70°C.

2.3. 5' RACE PCR. Synthesis of double stranded cDNA from mRNA

Two micrograms of mRNA were reverse transcribed using random hexameric primers (Promega) and MMLV reverse transcriptase

*Corresponding author. Fax: (33) (4) 93 95 77 04.

E-mail: barhanin@unice.fr or ipmc@unice.fr

Superscript-II (Life Technologies) for 1 h at 42°C. The second strand replacement synthesis was carried out using RNase H and DNA polymerase I for 2 h at 14°C. After blunt ending with T4 DNA polymerase, the double stranded cDNA was precipitated, and ligated to adaptors (5'-GATTTAGGTGACACTATAGAATCGAGGT-CGACGGTATCCAGTCCGACGAATTC-3') containing the Sp6 and KS sequences and *Sall* and *EcoRI* restriction sites (prepared by Dr. R. Waldmann in the laboratory).

2.4. Amplification of the 5' cDNA

A first PCR reaction using Sp6 primer (5'-GATTTAGGTGACACTAT-3') and a reverse primer corresponding to bp 623–641 on the cDNA sequence (5'-TGTGGTGGAGCACGGTGCTG-3') was followed by a second amplification using internal primers KS (5'-TA-GAATCGAGGTGACGGTATC-3') and a reverse primer corresponding to bp 450–480 of the cDNA sequence (5'-GAAGC-GCCGCTTCAGCTTGCGCAGCTCCTG-3'). The following PCR profile was used: 94°C for 30 s, 50°C for 30 s, 72°C for 1 min, 40 cycles. For subcloning, the PCR product was blunted, digested with *EcoRI* restriction enzyme, then separated on a 0.8% low melting point gel. DNA was extracted from agarose with the Wizard PCR purification kit (Promega) and eluted in water. Fragments were subcloned into pBluescript II SK[−] and analyzed by sequencing. The experiment was repeated with the Advantage-GC KlenTaq polymerase mix (Clontech).

2.5. PCR analysis of a somatic cell hybrid panel

DNA from the CV panel of mouse×Chinese hamster somatic cell hybrids [18] was kindly provided by Yvonne Boyd of the MRC Mammalian Genetics Unit (Harwell, UK). A set of oligonucleotide primers (5'-GAGAAGGCAGAAATGGAACTG-3' and 5'-GACCTTAG-CATCCACATAACAA-3') amplified a 365 bp fragment from a mouse CBA/H DNA template, while no amplification product could be detected when hamster V79TOR DNA was used as template. PCR reactions were performed in 25 µl containing 50 ng of template DNA, 0.5 µg of each primer, 1.5 mM MgCl₂, and 0.25 units of Taq polymerase in 1×PCR buffer recommended by the manufacturer (EUROBIO, France). A 480 Perkin Elmer thermal cycler was used with the following PCR amplification conditions: 94°C for 3 min, followed by 35 cycles of 94°C for 30 s, 58°C for 30 s, and 72°C for 30 s. Half of the reaction was loaded on a 2% agarose gel and separated by electrophoresis.

2.6. Northern blot and Master blot analysis

Total RNA was isolated from neonate (3 days) and adult (8 weeks) 129 Sv/J mouse tissues or from total embryos [17]. Approximately 3 and 6 µg of poly(A)⁺ from tissues or embryos, respectively, were

separated by electrophoresis on a 1% agarose gel and transferred onto nylon membranes (Hybond N, Amersham). Blots and a mouse Master blot (Clontech) were probed with a ³²P-labeled fragment of the TWIK coding sequence in Express Hyb solution (Clontech) at 65°C for 16 h, and washed stepwise to a final stringency of 0.2×SSC, 0.3% SDS at 65°C. Washed blots were exposed to a screen for Fuji Film Bio-Imaging analyzer BAS-1500 in order to quantify signals and then to X-OMAT AR film (Kodak, 8 days). Blots were stripped and reprobed using a β-actin probe to control for the variation in RNA loading. For each blot, the relative levels of transcripts were quantified and normalised to the level of β-actin and time of exposure.

2.7. Reverse transcriptase PCR (RT-PCR)

Five micrograms of total RNA from various adult mouse tissues were hybridized to random hexamers (Promega), and the RT reaction was carried out using MMLV reverse transcriptase (Life Technologies) for 1 h at 42°C. The forward (5'-AGCGTGTCCACCGTG-CATGTC-3') primer (position 751–770 on the TWIK cDNA sequence) and the reverse (5'-AATGGATGCAGTCAAGACTC-3') primer (position 1322–1341) were designated to amplify a 591 bp fragment. The following PCR profile was used: 94°C for 30 s, 55°C for 30 s, 72°C for 30 s, 34 cycles. Amplified products were separated by electrophoresis on a 1.5% agarose gel. GAPDH primers were used to control cDNA samples.

3. Results

3.1. Structure of the *twik* gene in the mouse

Seven genomic clones hybridizing with the TWIK cDNA were isolated and their insert DNA was analyzed by a combination of enzyme restriction digestion, Southern blotting and sequencing. The entire coding sequence of TWIK was found to be divided into three exons spanning over 30 kbp (Fig. 1A). The first exon identified is the only exonic region found in 25–30 kbp of genomic sequence spanning two overlapping λ clones. This exon is 547 bp long and contains the 5' untranslated region (UTR) as well as the translated sequence that corresponds to the cytoplasmic amino-terminus domain, the first transmembrane domain (M1) and the large extracellular loop M1P1 that is a common feature of all members of this channel family (Fig. 1A, Fig. 2B). The two other exons are separated by an intron of 3.6 kbp. The distance separating these exons and the first one was not established since they

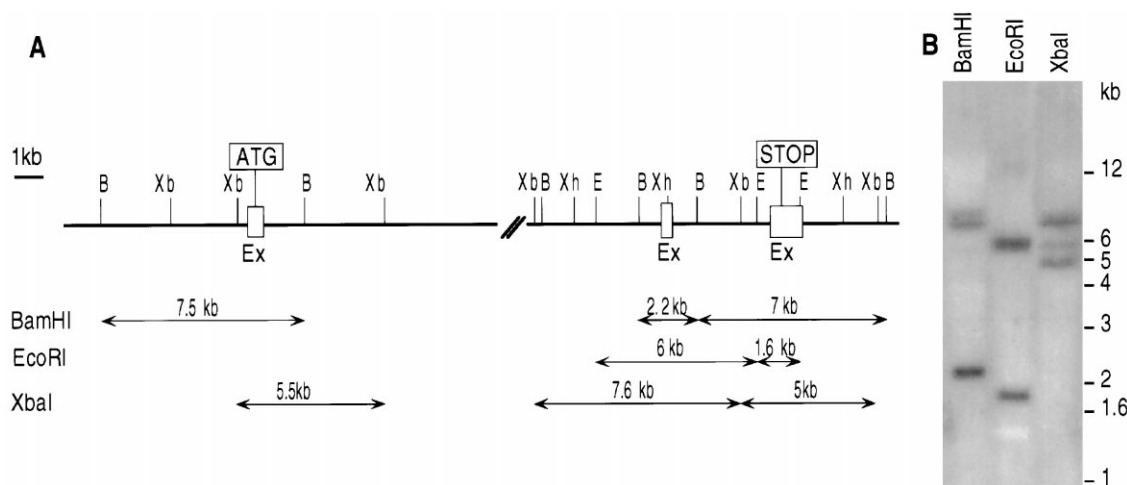
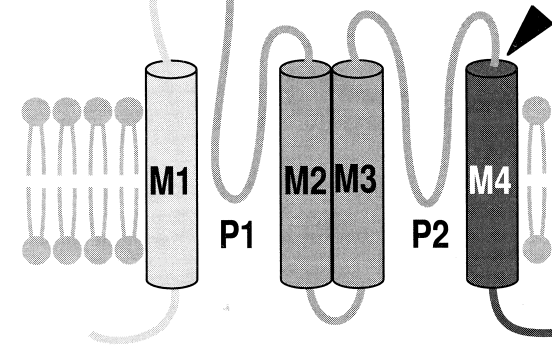


Fig. 1. The mouse *twik* gene. A: Low resolution map of two 14 kbp fragments of the mouse *twik* gene. Boxes represent the exons. 'ATG' and 'STOP' indicate the relative positions of the translation initiation and termination codons respectively. The position of sites for restriction enzymes is shown (B, *Bam*HI; E, *Eco*RI; Xb, *Xba*I; Xh, *Xho*I). The *Bam*HI, *Eco*RI and *Xba*I fragments that correspond to the bands revealed in the Southern blot of panel B are represented. B: Southern blot analysis of 129 Sv/J mouse genomic DNA. 20 µg of restriction enzyme digested genomic DNA was loaded per lane. Blot was probed at high stringency with a fragment of mouse TWIK cDNA containing the whole coding sequence.

B



The diagram shows a cross-section of the MscL channel. It consists of four subunits: M1 (light gray), M2 (dark gray), M3 (dark gray), and M4 (light gray). M1 and M4 are connected by a loop labeled P1, and M2 and M3 are connected by a loop labeled P2. The subunits are embedded in a lipid bilayer. Two black arrowheads point to the loops P1 and P2, indicating their putative role in the channel's function.

main (M4), the cytoplasmic carboxy tail and the 3' UTR. The sequences at the exon-intron boundaries are shown in Fig. 2 and match with the consensus sequences of splice junctions [19]. A Southern blot analysis of genomic DNA isolated from liver of 129 Sv/J mice was performed in order to verify the

Table 1
Chromosomal assignment of *twik* with a mouse/hamster somatic cell hybrid panel

Hybrid	Mouse chromosome																				<i>twik</i>	
	1	2	3	4	5	6	7	8	9	10	11	12	13	14	15	16	17	18	19	X		Y
CV1	+	–	–	–	–	–	–	(+)	–	–	–	–	–	+	–	+	–	+	–	+	+	+
CV1/1/1	–	–	–	–	–	+	+	–	–	–	–	–	+	+	–	+	+	–	–	+	–	–
CV1/3/1/1	–	–	–	–	–	+	+	–	–	–	–	–	+	+	–	+	–	–	–	+	–	–
CV3	–	–	+	–	–	+	+	–	–	–	–	–	+	+	–	+	+	–	+	+	+	–
CV3/1/1/1	–	–	+	–	–	+	+	–	–	–	–	–	+	+	–	+	–	–	+	+	+	–
CV3/2/1/1	–	–	–	–	–	–	+	–	–	–	–	–	+	+	–	+	–	–	–	+	+	–
CV3/3/1/1	–	–	+	–	–	+	+	–	–	–	–	–	+	+	–	+	+	–	+	+	+	–
CV4	+	+	–	+	–	+	–	–	–	–	–	–	+	+	+	–	+	–	–	+	+	+
CV4/1/1/1	+	+	–	+	–	+	–	–	–	–	–	–	–	+	+	–	+	–	–	+	+	–
CV4/2/1/1	+	–	–	+	–	+	–	–	–	–	–	–	–	+	+	–	+	–	–	+	+	–
CV7	–	+	–	+	–	+	+	–	–	–	–	–	+	+	–	+	+	–	–	+	+	–
CV7/1/1/1	+	–	–	–	–	–	–	–	–	–	–	–	–	+	–	+	–	–	–	+	+	–
CV7/2/1/1	+	–	–	–	–	–	–	–	–	–	–	–	–	+	–	–	–	–	–	+	+	–
CV7/3/1/1	+	–	–	–	–	–	–	–	–	–	–	–	–	–	–	+	–	–	–	+	+	–
CV8	+	+	–	+	–	+	+	+	–	+	–	+	+	+	+	–	–	–	+	+	+	+
CV8/1/1/1	+	+	–	+	–	+	+	+	–	+	–	+	+	+	+	–	+	–	+	+	+	+
CV8/2/1/1	–	+	–	+	–	+	+	+	–	+	–	+	+	+	+	–	–	–	–	+	–	+
CV10	–	–	+	–	–	+	+	+	–	–	–	–	–	+	–	±	–	+	–	+	+	+
CV10/1/1/1	–	–	–	–	–	+	+	+	–	–	–	–	+	+	–	+	+	+	–	+	+	+
CV10/2/1/1	–	–	+	–	–	+	+	–	–	–	–	–	–	+	–	–	+	+	–	+	+	–
CV10/3/1/1	–	–	–	–	–	+	+	–	–	–	–	–	+	+	–	+	+	+	–	+	+	–
CV10/3/1/1R	–	–	–	–	–	–	–	–	–	–	–	–	+	+	–	+	–	+	–	–	+	–
MOV11/2/4/1	±	–	+	+	+	+	+	–	–	–	–	–	+	–	–	–	–	+	+	–	–	–
MOV11/3/1/2	+	(+)	+	+	+	+	+	–	+	–	–	–	+	–	–	–	+	+	+	+	–	+
Discordance	8	5	11	7	7	12	12	2	7	6	8	5	13	15	6	17	12	8	9	15	15	

The table shows the mouse chromosome content of each hybrid cell line, '+' and '–' indicate presence or absence respectively of the chromosome; (+) indicates that the chromosome is present in only a portion of the cells; (±) indicates that inconsistent results have been observed in PCR experiments. The presence or absence of the 365 bp PCR product specific for the *twik* gene is indicated in the '*twik*' column. The discordance value between the experimental and theoretical results for each chromosome is given in the bottom line.

restriction map analysis and to determine the copy number of the *twik* gene in the mouse genome. Each digestion produced the bands of the predicted size and no extra bands were detected. This result demonstrates that *twik* is present in a single gene copy in the mouse (Fig. 1B).

3.2. Chromosomal localization of the mouse *twik* gene

The CV panel of mouse×Chinese hamster somatic cell hybrids was used for chromosomal assignment of the mouse *twik* gene [18]. A primer set was derived from the *twik* gene in order to amplify a 365 bp fragment from mouse genomic DNA (CBA/H), while no amplification product could be obtained from genomic hamster DNA (V79TOR). Out of the 24 hybrid lines tested, eight gave a PCR product at the expected size. The chromosome content of these hybrids as well as the results of the PCR amplification are reported in Table 1. The discordance ratio for each chromosome was calculated and the lowest value (2/24) is consistent with mapping of the *twik* gene to mouse chromosome 8.

3.3. Transcriptional initiation sites of the *twik* gene

In an attempt to localize the promoter region of the mouse *twik* gene, we first identified the transcriptional start sites using 5' RACE-PCR. Two rounds of PCR were carried out from brain cDNA by using nested primers. The amplified products were subcloned and eight clones containing an insert that hybridized to an internal TWIK cDNA specific oligonucleotide were isolated and sequenced. The 5' sequences of these clones start at positions 2, 4, 8, 24, 31, 32 and 65 of the TWIK cDNA sequence (GenBank accession number AF033017). Therefore, no additional sequence to the previously known 5' UTR has been unveiled [16]. These minor

differences in the 5' sequence could reflect the use of multiple transcription start sites. This conclusion is in agreement with the fact that the length of the TWIK cDNA (2240 bp) corresponds to the size of the major TWIK transcript, as evaluated by Northern blot analysis (around 2.2 kbp, see Fig. 4). The analysis of the genomic 5' sequence flanking the first exon does not reveal the presence of TATA or CAAT boxes or of other usual functional initiator elements [20,21] close to the putative start site. No further attempt to identify the promoter region was made.

3.4. Tissue distribution of TWIK mRNA

The expression of TWIK in various adult mouse tissues was analyzed by hybridizing a mouse Master blot from Clontech (Fig. 3A) and by non-quantitative RT-PCR (Fig. 3C). Expression levels determined by hybridization and RT-PCR from the same tissues were consistent: in both cases, expression of TWIK was found to be very low in heart and skeletal muscle, moderate in the thymus and abundant in salivary gland and uterus. By compiling results from both experiments, tissues can be classified in three groups according to their relative levels of TWIK expression. TWIK mRNA is abundant in the brain, kidney, thyroid, salivary and adrenal glands, prostate, epididymis, uterus, placenta, colon and jejunum. TWIK is expressed at more moderate levels in eyes, pituitary, pancreas, smooth muscle, ovary and testis. Tissues such as lung, aorta, liver, heart, skeletal muscle, thymus and spleen display poor to very poor expression.

3.5. Developmental expression of TWIK mRNA

Interestingly, the TWIK message was detected as soon as day 7 during mouse development (Fig. 3A). The Northern

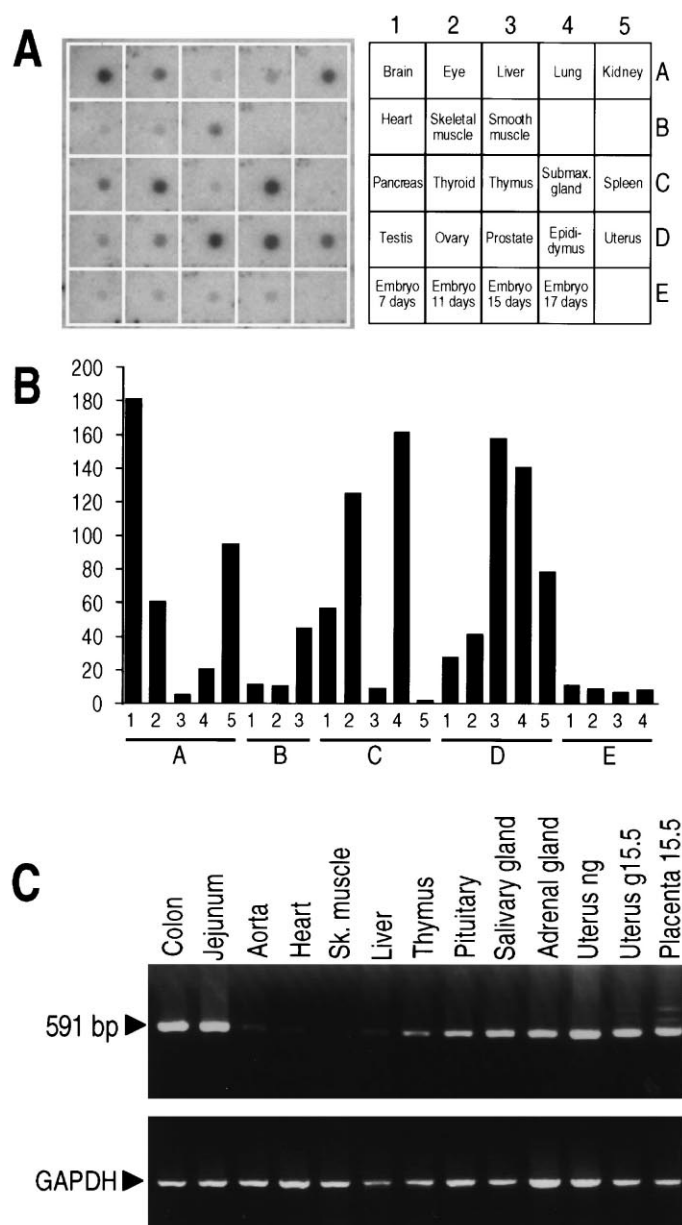


Fig. 3. Expression of TWIK in mouse tissues. A: Hybridization of a TWIK probe to a mouse RNA Master blot. Each dot corresponds to 100–500 ng of poly(A)⁺ RNA. B: Relative expression of TWIK mRNA in various mouse tissues. C: Ethidium bromide stained gel showing RT-PCR analysis of TWIK expression in various mouse tissues. Primers were deduced from sequences present in exon 2 and exon 3. The amplified fragment is 591 bp long. A GAPDH fragment was amplified as control.

blot shown in Fig. 4A indicates that a TWIK transcript of 2.2 kbp is present in mRNA isolated from whole 11.5 day (pc) embryos. The relative quantification achieved using a Fujifilm Bio-Imaging analyzer reveals that only a small increase of the 2.2 kbp TWIK message takes place from day 11.5 to day 18.5 (Fig. 4C). A similar increase of TWIK expression can be quantified on the dot blot (Fig. 3C). TWIK was also found to be present at a completely undifferentiated stage because it was amplified by RT-PCR from embryonic stem cells (not shown).

In adult mice, the TWIK message is particularly abundant in brain and kidney and moderately abundant in lung (Fig. 4B). The levels of TWIK mRNA expression in these three tissues were compared in neonate and adult 129 Sv/J mice

(Fig. 4B). As in embryos, a band at 2.2 kbp was detected in the three tissues with the following order of intensities in neonates: kidney > brain > lung. An additional band of ~2.4 kbp was also present in brain mRNA at both stages, which represented approximately half of the specific signal (Fig. 4B,C). This transcript heterogeneity could arise from alternative splicing or multiple sites of polyadenylation. The most likely hypothesis is a difference in the 3' UTR since both RT-PCR and 5' RACE-PCR failed to reveal extra sequences in the 5' UTR and in the coding region. A large increase of the amount of TWIK transcripts occurs in brain from neonate to adult stages (5-fold) while in kidney and lung, the transcript levels only double during the same development period (Fig. 4B,C). As a consequence, the brain is the

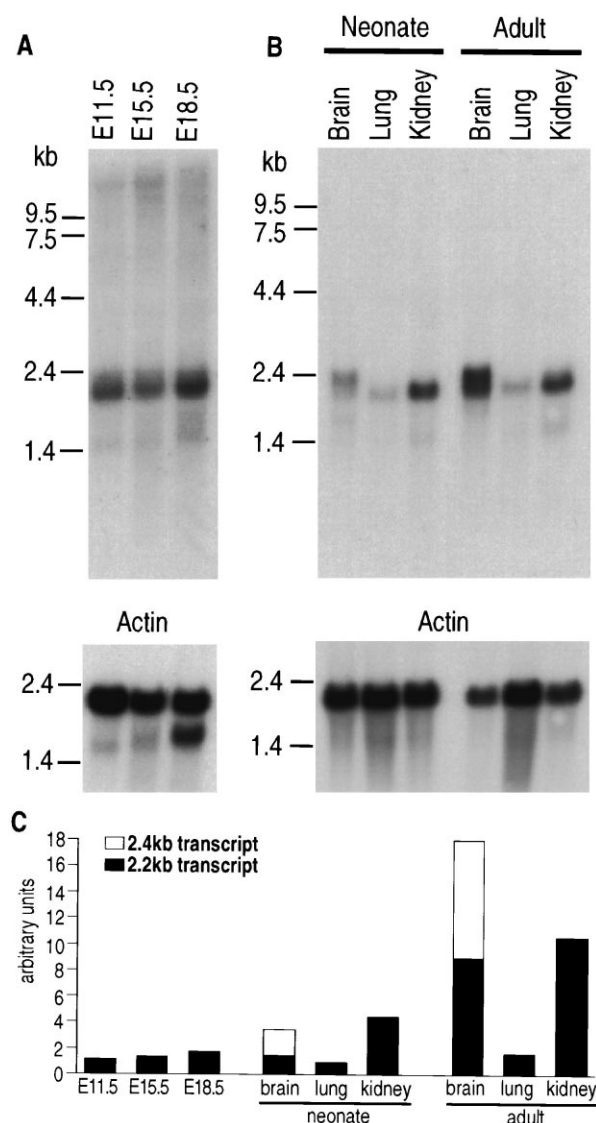


Fig. 4. Northern blot analysis of TWIK expression in mouse embryos and adult tissues. RNA was prepared from total embryos (A) and from neonate and adult tissues (B). 3 µg (A) and 6 µg (B) of poly(A)⁺ RNA were loaded per well. The probe used consisted of the TWIK coding region. Autoradiograms were exposed for 8 days. For controls, blots were reprobated with β-actin. The diagram in C represents the relative levels of TWIK transcripts normalized by β-actin and time of exposure.

tissue that express the highest level of TWIK mRNA in the adult mouse.

4. Discussion

In this paper, we have determined the genomic organization of TWIK, its chromosomal localization, as well as its tissue distribution during development. We cloned and partially sequenced large fragments of the mouse *twik* gene. Analysis of these fragments demonstrates that the TWIK coding sequence is contained within three exons. The *twik* gene appears to have a size considerably larger than the exonic sequence (around 2.2–2.4 kbp) because the size of introns is relatively high, especially the first intron which is larger than 25–30 kbp. With the gene structure of the TWIK channel being charac-

terized, it would have been interesting to identify the promoter elements related to the transcriptional control of its expression in different tissues. As a first step to this investigation, the transcriptional initiation sites were determined by using the 5' RACE-PCR technique. No additional transcribed sequences compared to the previously cloned cDNA were found. Instead, this study confirmed the cDNA clone as a full length clone. However, no well characterized core-promoter elements were found in the genomic 5' sequence that flanks the potential transcriptional initiation sites. Although the size of the cDNA that we isolated is in agreement with the RNA transcript size seen on Northern blot, it cannot be totally excluded that a small additional exonic sequence has escaped our investigation. Such a hypothesis is made likely by the fact that a stretch of 52 pyrimidines adjacent to the exon 1 could correspond to a splice site [22].

We assigned the *twik* gene to the mouse chromosome 8 using a mouse/hamster somatic cell hybrid panel. This result is consistent with the localization of the human TWIK gene to chromosome 1q42–43 [23]. This region of the human genome has been reported to form a conserved linkage group with distal mouse chromosome 8 [24].

The expression of TWIK mRNA in some adult mouse tissues was previously examined by Northern blot analysis [16]. In this work, we have extended this study to many other tissues by hybridizing a mouse Master blot and by RT-PCR. It appears that TWIK is widely distributed in the mouse. Since virtually all living cells maintain a more or less negative membrane potential, such a wide distribution is expected with regard to the supposed function of TWIK associated with the background permeability to K⁺ ions. The brain is one of the richest sources of TWIK transcripts and its abundance is 5-fold higher at the adult stage compared to neonate. As immunocytochemistry studies have suggested a synaptic localization of the TWIK protein in several brain areas (Inger Lauritzen, personal communication), it is likely that the TWIK brain messenger augmentation parallels the synaptogenesis, as has already been found for other K⁺ channels [25]. In developing mouse embryos, TWIK transcripts are detected at embryonic stages as early as day 7 pc. In fact, a PCR experiment run on embryonic stem cell cDNA revealed that TWIK messengers are already found in these totally undifferentiated cells (not shown).

This work represents the first analysis of the *twik* gene, as well as its temporal expression in mouse tissues. This information will be useful in the execution and interpretation of targeting experiments designed to elucidate the functional role of TWIK channels in vivo. Given the high identity (94%) between human and mouse amino acid sequence of TWIK, results obtained from a gene targeting experiment in the mouse should provide insight into the role of TWIK in other mammals and particularly in humans.

Acknowledgements: We are grateful to Yvonne Boyd for providing DNAs of the somatic cell hybrid panel and for Drs. Marc Borsotto, Christian Dani, Amanda Patel and Rainer Waldmann for very fruitful discussions. Thanks are due to Maud Larroque, Nathalie Leroudier, Franck Aguila and Dahvya Doume for technical assistance. This work was supported by the Centre National de la Recherche Scientifique (CNRS), the Association Française contre les Myopathies (AFM) and the Association pour la Recherche sur le Cancer (ARC, G.F.C.).

References

- [1] Rudy, B. (1988) *Neuroscience* 25, 729–749.
- [2] Hille, B. (1992) *Ionic Channels of Excitable Membranes*, 2nd edn., Sinauer, Sunderland, MA.
- [3] Pongs, O. (1992) *Trends Pharmacol. Sci.* 13, 359–365.
- [4] Jan, L.Y. and Jan, Y.N. (1994) *Nature* 371, 119–122.
- [5] Chandy, K.G. and Gutman, G.A. (1995) in: *Ligand and Voltage-Gated Ion Channels* (North, R.A., Ed.), pp. 1–71, CRC, Boca Raton, FL.
- [6] Barhanin, J., Lesage, F., Guillemare, E., Fink, M., Lazdunski, M. and Romey, G. (1996) *Nature* 384, 78–80.
- [7] Kohler, M., Hirschberg, B., Bond, C.T., Kinzie, J.M., Marrion, N.V., Maylie, J. and Adelman, J.P. (1996) *Science* 273, 1709–1714.
- [8] Patel, A.J., Lazdunski, M. and Honoré, E. (1997) *EMBO J.* 16, 6615–6625.
- [9] Mackinnon, R. (1995) *Neuron* 14, 889–892.
- [10] Doupnik, C.A., Davidson, N. and Lester, H.A. (1995) *Curr. Opin. Neurobiol.* 5, 268–277.
- [11] Isomoto, S., Horio, Y., Matsumoto, S., Kondo, C., Yamada, M., Gilbert, D.J., Copeland, N.G., Jenkins, N.A. and Kurachi, Y. (1997) *Mamm. Genome* 8, 790–791.
- [12] Nichols, C.G. and Lopatin, A.N. (1997) *Annu. Rev. Physiol.* 59, 171–191.
- [13] Lesage, F., Guillemare, E., Fink, M., Duprat, F., Lazdunski, M., Romey, G. and Barhanin, J. (1996) *EMBO J.* 15, 1004–1011.
- [14] Fink, M., Duprat, F., Lesage, F., Reyes, R., Romey, G., Heurteaux, C. and Lazdunski, M. (1996) *EMBO J.* 15, 6854–6862.
- [15] Duprat, F., Lesage, F., Fink, M., Reyes, R., Heurteaux, C. and Lazdunski, M. (1997) *EMBO J.* 16, 5464–5471.
- [16] Lesage, F., Lauritzen, I., Duprat, F., Reyes, R., Fink, M., Heurteaux, C. and Lazdunski, M. (1997) *FEBS Lett.* 402, 28–32.
- [17] Vetter, D.E., Mann, J.R., Wangemann, P., Liu, J.Z., McLaughlin, K.J., Lesage, F., Marcus, D.C., Lazdunski, M., Heinemann, S.F. and Barhanin, J. (1996) *Neuron* 17, 1251–1264.
- [18] Williamson, P., Holt, S., Townsend, S. and Boyd, Y. (1995) *Mamm. Genome* 6, 429–432.
- [19] Mount, S.M. (1982) *Nucleic Acids Res.* 10, 459–472.
- [20] Weis, L. and Reinberg, D. (1992) *FASEB J.* 6, 3300–3309.
- [21] Roeder, R.G. (1996) *Trends Biochem. Sci.* 21, 327–335.
- [22] Goux, P.M., Libri, D., d'Aubenton, C.Y., Fiszman, M., Brody, E. and Marie, J. (1990) *EMBO J.* 9, 241–249.
- [23] Lesage, F., Mattei, M.G., Fink, M., Barhanin, J. and Lazdunski, M. (1996) *Genomics* 34, 153–155.
- [24] Abonia, J.P., Abel, K.J., Eddy, R.L., Elliott, R.W., Chapman, V.M., Shows, T.B. and Gross, K.W. (1993) *Mamm. Genome* 4, 25–32.
- [25] Lesage, F., Attali, B., Lazdunski, M. and Barhanin, J. (1992) *FEBS Lett.* 310, 162–166.